Huda A.J. Mohammed
Ruba F. Abbas
Ali A. Waheb
Mohammed J.M. Hassan

Department of Chemistry,
College of Science,
Mustansiriyah University,
Baghdad, IRAQ

One-Step Green Sonochemical Co-Precipitation Synthesis of Co-Doped Fe_3O_4 Nanoparticles for Improved Photoluminescence

In this study, a simple and single-step sonochemical co-precipitation method used for the synthesis of cobalt-doped Fe_3O_4 magnetic nanoparticles at room temperature. This new method is environmentally friendly used ultrasound irradiation to control the morphology and growth of MNPs, minimizing the use of high temperatures and toxic chemicals. Both of Fe_3O_4 and Co_3O_4 phases are confirmed by the XRD analysis, with an average crystallite size of 10.9 ± 0.5 nm. A spherical morphology of the synthesized nanoparticles is revealed by FE-SEM images with an average particle size of 33.26 nm. EDX and mapping confirmed Fe, Co, and O presence. Photoluminescence (PL) studies showed increased PL intensity for the synthesized nanoparticles compared to undoped Fe_3O_4, due to enhanced surface defects, light absorption, and surface area. The broader 3D pL excitation spectrum of Co_3O_4 in the doped nanoparticles was investigated. These results indicate that this method is simple procedure used to prepare Co-doped Fe_3O_4 nanoparticles with improved photoluminescence properties for applications in bio imaging, drug delivery, sensing, data storage, and environment treatment.

Keywords: Green synthesis; Magnetite; Sonochemical co-precipitation; PL
Received: 3 February 2025; **Revised:** 8 April; **Accepted:** 15 April 2025

1. Introduction

Magnetic nanoparticles have arisen as very important materials in recent decades due to their wide-ranging applications, including chemistry, engineering, acoustics, magnetic hydrodynamics, physics, biotechnology/biomedicine, computational modeling, water purification, heavy metal removal, and other applied sciences [1-3]. Doping magnetic nanoparticles (DMNPs) with cobalt (Co) or manganese (Mn) shows a powerful approach to improve their performance. Such doping modifies surface properties, improving their chemical reactivity, and can also increase magnetic field strength, potentially leading to superparamagnetic behavior [4-6]. Cobalt-doped magnetite ($Co_xFe_{3-x}O_4$) is one of DMNPs a material has used in various applications, particularly those leveraging its optical and magnetic properties [7,8]. Traditional synthetic methods for nanoparticles often involve the use of hazardous chemicals, high temperatures, and cruel reaction conditions, raising environmental concerns. Therefore, the synthesis of nonmaterial with cost-effective, environmentally benign, and energy-efficient methodologies is considered green synthesis. The one of green synthesis is sonochemical method, which harnesses the power of ultrasound for synthesis nanoparticles. This method offers several advantages, such as lower energy consumption, decreased reliance on harmful solvents, and controlling nanoparticle morphology and growth [9-11]. The combination of sonochemical synthesis with the co-precipitation method at room temperature, without heating, further increases these advantages. The ultrasonic technique provides control over the morphology and particle size of the resulting nanoparticles [12]. Furthermore, the room-temperature approach reduces costs, minimizes energy requirements, and it's more environmentally friendly. The use of less toxic or even water-based solvents, the suppression of side reactions, and of fewer solvents all contribute to minimizing environmental impact, making this method greener and simpler [13]. The photoluminescence (PL) properties of Co-doped Fe_3O_4 MNPs are influenced by the creation of defects in the crystal lattice. These defects introduce new energy levels within the band gap, which can act as traps for electrons or holes, thereby influencing the way the MNPs interact with emit and absorb light [14]. Doping Fe_3O_4 MNPs can either enhance or quench PL intensity, depending on the dopant element. In the case of cobalt (Co) doping, an increase in PL intensity is typically observed [15]. This enhanced luminescence opens up exciting possibilities for applications in areas such as medical, bio imaging, and sensing. This study explores the green sonochemical synthesis of Co-doped Fe_3O_4 MNPs, characterizing their structural, morphological, and photoluminescence properties to understand the influence of cobalt doping on their performance.

2. Experimental Part

All chemicals were high purity and used directly without purification. Beam Gostar Taban Company in Tehran, Iran, conducted characterization of the surface properties of the Co-doped Fe_3O_4 MNPs.

A co-precipitation method was employed to synthesize Co-doped Fe_3O_4 MNPs. Initially, 25 mL of 0.8 M $FeCl_3$ (≥99.0%) and 25 mL of 0.4 M $FeCl_2$ (≥99.0%) were combined under vigorous magnetic

stirring (500 rpm) for 30 minutes at room temperature to homogenize the (Fe^{2+}/Fe^{3+}=1:2) solution. Subsequently, 25 mL of 0.4 M $Co(NO_3)_2 \cdot 6H_2O$ (≥98.0%) was introduced into the mixture, followed by continuous magnetic stirring for 30 minutes to ensure uniform incorporation of cobalt ions. The resultant solution was then subjected to probe ultrasonication (20 kHz, 50% amplitude) for 30 minutes to reduce agglomeration and facilitate nanoparticle nucleation. For precipitation MNPs, 75 mL of 5 M NaOH (≥97.0%) was added dropwise (1–2 mL/min) to the stirred solution until a black-brown precipitate formed, indicating the formation of MNPs. The suspension was stirred for an additional 30 minutes to complete the reaction. The MNP precipitate was separated and washed numerous times with deionized water until the supernatant reached neutral pH, and dried at 60°C for 6 hours (Fig. 1). To prepare undoped Fe_3O_4 nanoparticles, all steps were repeated without the addition of $Co(NO_3)_2 \cdot 6H_2O$.

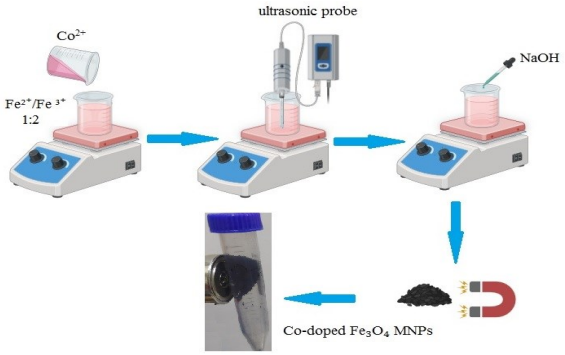

Fig. (1) Scheme of synthesis Co-doped Fe_3O_4 MNPs using sonochemical co-precipitation method

3. Results and Discussion

The formation of cobalt-doped magnetite ($Co_xFe_{3-x}O_4$) depends on the Schikorr reaction, which describes the formation of magnetite (Fe_3O_4) through the following reactions [16]:

First: Dissociation of iron salts in water:

$FeCl_3$ (aq) → Fe^{3+} (aq) + $3Cl^-$ (aq)

$FeCl_2$ (aq) → Fe^{2+} (aq) + $2Cl^-$ (aq)

Second: Reaction with NaOH:

Fe^{3+}(aq) + $3OH^-$(aq) → $Fe(OH)_3$ (s) (Ferric Hydroxide)

Fe^{2+}(aq) + $2OH^-$(aq) → $Fe(OH)_2$ (s) (Ferrous Hydroxide)

Third: The iron hydroxides react to form magnetite (Fe_3O_4):

$2Fe(OH)_3$(s) + $Fe(OH)_2$ (s) → Fe_3O_4 (s) + $4H_2O$ (l)

The Schikorr reaction is a simultaneous reduction-oxidation reaction where $Fe(OH)_3$ is reduced to Fe^{2+} ions while $Fe(OH)_2$ is oxidized to Fe^{3+} ions, leading to the formation of Fe_3O_4.

After cobalt doping, the reaction becomes:

$xCoCl_2$ (aq) + $2FeCl_3$ (aq) + $(1-x)FeCl_2$ (aq) + 8NaOH (aq) → $Co_xFe_{3-x}O_4$ (s) + 8NaCl (aq) + $4H_2O$ (l)

where 'x' represents the amount of cobalt incorporated. However, the basic Schikorr reaction remains the core process for the formation of the Fe_3O_4 component, even when cobalt is incorporated into the Fe_3O_4 structure

X-ray diffraction (XRD) with a Shimadzu XRD-6000 diffractometer was employed to analyze the crystalline structure of the produced nanoparticles. Measurements were conducted under Cu Kα radiation (λ = 1.54 Å) across a 2θ angular range of 10°–80°.

The Debye-Scherrer formula was used to estimate the crystallite size [17]:

$$D = \frac{k\,\lambda}{\beta cos\theta} \qquad (1)$$

where D represents the crystallite size, λ is the X-ray wavelength (1.54 Å), k is the Scherrer constant, β or FWHM denotes the full width at half maximum of the diffraction peak, and θ is the diffraction angle

The calculated crystallite size averaged 10.9±0.5 nm, consistent with nanoscale dimensions, as derived from the (311) reflection of the magnetite phase (Fe_3O_4). The XRD pattern of Co-doped Fe_3O_4 MNPs MNPs synthesized by co-precipitation method shows the diffraction peaks at 2θ = 18.36°, 30.27°, 35.62°, 43.12 °, 53.28 °, 57. 02 °, and 62.51° corresponding to crystal planes of (111), (220), (311), (400), (422), (511), and (440), this indicates that the crystalline structure of Fe_3O_4 MNPs can remain after combining with Co_3O_4. Six peaks of Co_3O_4 appeared at 18.36° (111), 30.27° (220), 35.62° (311), 39.18 ° (222), and 43.12° (400) [18]. Two peaks appearing at 24° and 46.7° are not from a single phase but rather from the combined contributions of Fe_3O_4 and Co_3O_4 due to overlapping peaks. This is a common phenomenon in mixed-phase nanomaterials with spinel crystal structures of Fe_3O_4 and Co_3O_4 (Fig. 2).

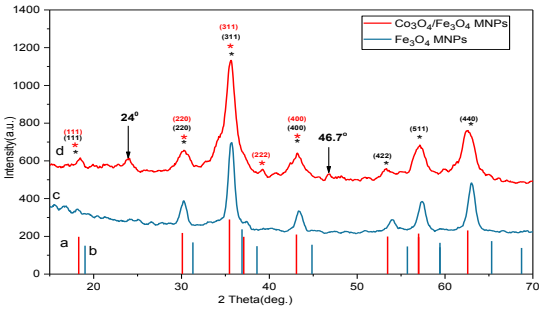

Fig. (2) XRD patterns of: (a) red line is the code of AMCSD 0007824, (b) blue line is the code of AMCSD 0007469, (c) Fe_3O_4 MNPs, and (d) Co-doped Fe_3O_4 MNPs using sonochemical co-precipitation method

Energy-dispersive x-ray spectroscopy (EDX) analysis offers quantitative and qualitative knowing insights into the elements present in the sample [19]. In this study, EDX with a JEOL JSM-6510 LV instrument (Japan) was used to determination of the elemental composition of the cobalt-doped Fe_3O_4 MNPs. Figure 3 shows that the iron, cobalt, and oxygen were detected, indicating these elements effective distribution within nano sample. The element type and its oxidation state

were detected by the energy level of each peak of EDX. In the spectrum of Figure 3, the iron peaks refer to the Fe^{3+} state (characteristic of iron in magnetite). In the spectrum, the presence of iron in multiple oxidation states (Fe^{2+} and Fe^{3+}) were appeared at 0.7 keV and 6.4 keV. Moreover, the presence of cobalt in two different oxidation state (Co^{2+} and Co^{3+}) were found at 6.9 keV and 7.5 keV. A single peak was also observed for oxygen [20].

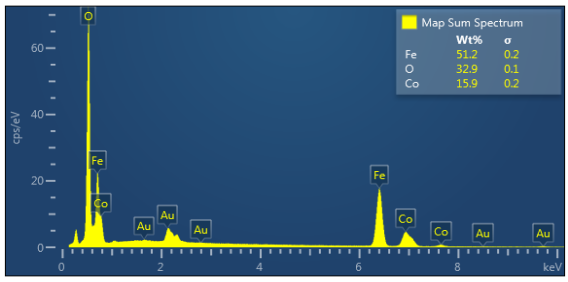

Fig. (3) EDX spectra of the Co-doped Fe_3O_4 MNPs

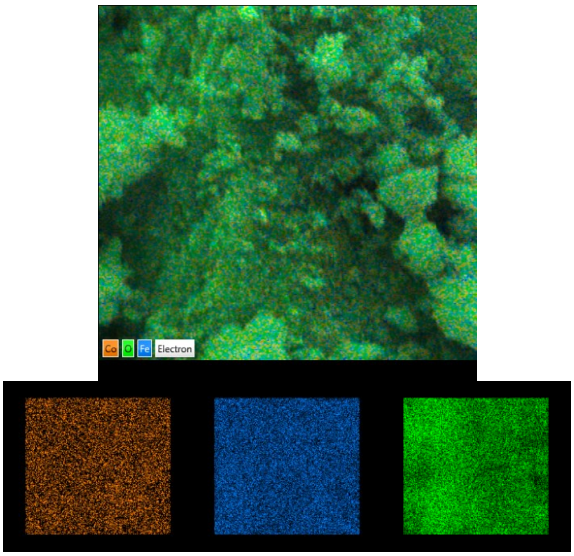

Fig. (4) EDX mapping of Co-doped Fe_3O_4 MNPs

The visual representation of elemental distribution across the sample is creates by EDX mapping technique [21]. The comparison of copper, iron, and oxygen in the nonmaterial distribution patterns before and after the diffusion process is shown in Fig. (4). The morphology of the surface and composition of nano samples is study by using JEOL JSM-6510 LV field-emission scanning electron microscope (FE-SEM) [22]. FE-SEM images revealed that the Co-doped Fe_3O_4 MNPs exhibited a spherical morphology and shape (Fig. 5). The average size of the Co-doped Fe_3O_4 MNPs was determined to be 33.26 nm by using Gaussian fit of size distribution.

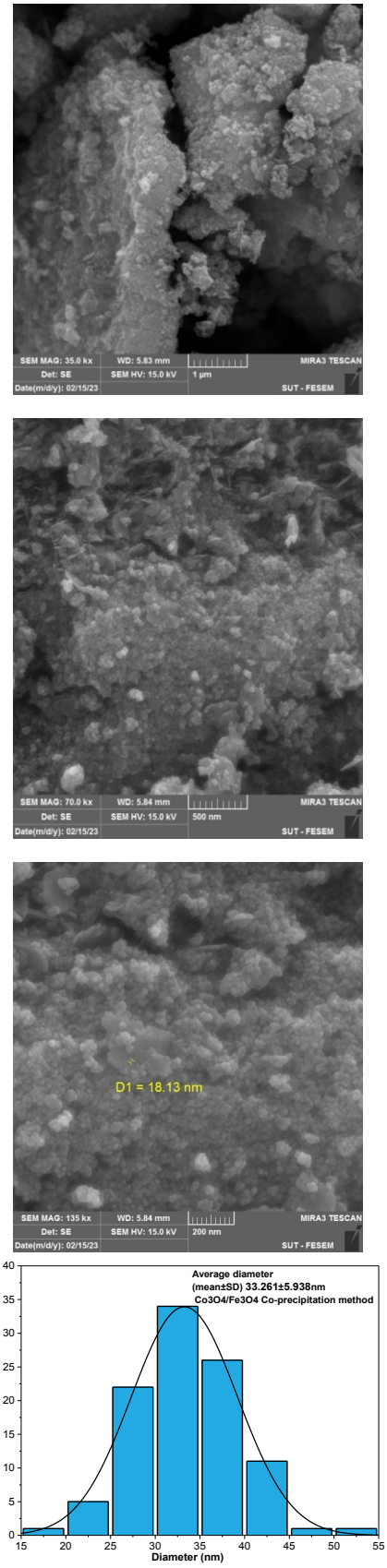

Fig. (5) FE-SEM image at 10 µm, 500 nm, and 200 nm, and histogram of particle size distribution for Co-doped Fe_3O_4 MNPs

Photoluminescence (PL) analysis is a technique used to investigate the energy levels and electronic transitions and in nanomaterial. In this technique, the nanomaterial is excited with light of a specific wavelength, and then the emitted light from the nanomaterial is analyzed [23]. The intensity and emitted light's wavelength provide information about the material's defect states and band gap [24,25]. The PL measurements were conducted using a PerkinElmer LS55 spectrometer (Germany). The PL intensity of the Co_3O_4/Fe_3O_4 MNPs was observed to be higher than that of the Fe_3O_4 MNPs. This is due to the higher surface area of Co_3O_4/Fe_3O_4 MNPs compared to Fe_3O_4 MNPs, which means that there are more active sites for photo-excitation and PL emission. On the other hand, the addition of Co_3O_4 to Fe_3O_4 leads to increased light absorption, which results in a higher number of excited electrons, resulting in increased emission intensity. Moreover, the addition of Co_3O_4 to Fe_3O_4 increases surface defects. This leads to the reduced recombination of electron-hole pairs onto the surface of Co_3O_4/Fe_3O_4 MNPs, leading to stronger PL emission.

The energy gap can calculate by following [26]:

$$E_g(eV) = \frac{1240}{\lambda} \quad (2)$$

where λ is the wavelength of absorbed light (nm) and E_g is the energy gap

From Fig. (6), a maximum wavelength at 616 nm for both Co_3O_4/Fe_3O_4 MNPs and Fe_3O_4 and the value of energy gap is 2.01 eV. The comparison between the 3D PL excitation spectra of Co_3O_4/Fe_3O_4 MNPs and Fe_3O_4 MNPs can be observed in figures (7) and (8). Co_3O_4/Fe_3O_4MNPs show a broader range of excitation wavelengths due to Co_3O_4 can absorb a wider range of wavelengths compared to Fe_3O_4, while Fe_3O_4 MNPs have PL excitation spectrum more limited in specific range of excitation wavelengths. The quantum yield means the efficiency of photon emission per photon absorbed, the addition Co_3O_4 leads to increasing in the quantum yield due to the efficient energy transfer and a broader range of emission from Co_3O_4.

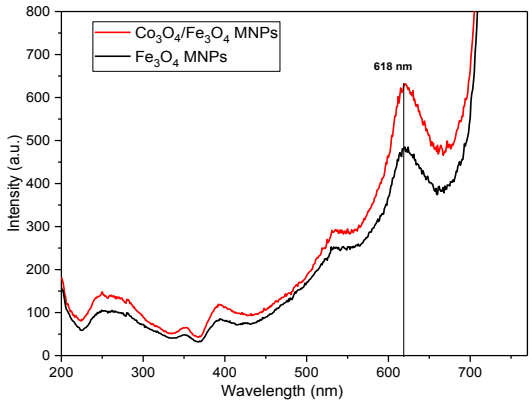

Fig. (6) PL excitation spectra of Co-doped Fe_3O_4 MNPs and Fe_3O_4 MNPs

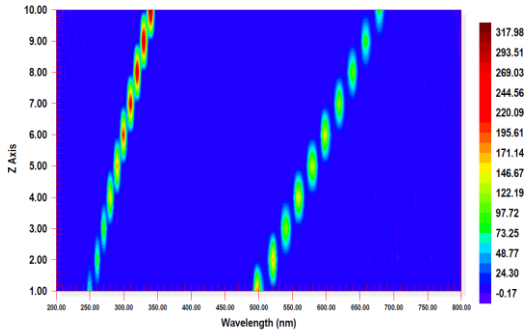

Fig. (7) 3D PL excitation spectra of Co-doped Fe_3O_4 MNPs

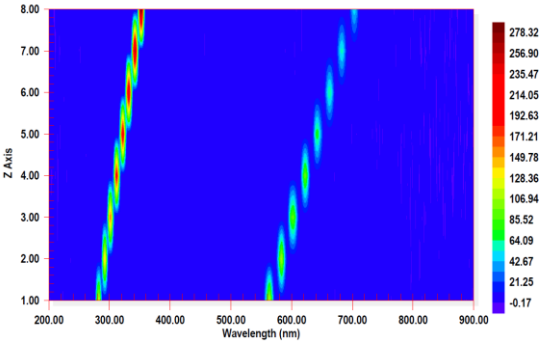

Fig. (8) 3D PL excitation spectra of Fe_3O_4 MNPs

4. Conclusion

The simple sonochemical co-precipitation method was successfully used to synthesize Co-doped Fe_3O_4 MNPs at room temperature in this study. The characterization results confirmed the successful incorporation of cobalt into the Fe_3O_4 lattice, leading to the formation of $Co_xFe_{3-x}O_4$ and successful controlling the size and morphology. The Co-doped Fe_3O_4 MNPs exhibited a considerably higher PL intensity compared to Fe_3O_4 MNPs due to an increase in active sites for photoexcitation and PL emission, resulting from the larger surface area of the Co-doped Fe_3O_4 MNPs. Moreover, the higher PL intensity of the Co-doped Fe_3O_4 MNPs is attributed to both increased light absorption and increased surface defects, due to a greater number of excited electrons and reduced electron-hole recombination. The energy gap of both materials is 2.01 eV at 616 nm. The above-mentioned properties suggest that this simple and green synthesis method is a promising alternative to traditional methods for further enhancing the PL properties and investigating the magnetic properties of the synthesized materials.

Acknowledgment

We thank the Department of Chemistry, College of Science at Mustansiriyah University for their help.

References

[1] P. Ryapolov et al., "Magnetic fluids: The interaction between the microstructure,

macroscopic properties, and dynamics under different combinations of external influences", *Nanomaterials*, 14(2) (2024) 222.

[2] R.F. Abbas, M.J.M. Hassan and A.M. Rheima, "Adsorption of fast green dye onto Fe_3O_4 MNPs and GO/Fe_3O_4 MNPs synthesized by photo-irradiation method: Isotherms, thermodynamics, kinetics, and reuse studies", *Sustain. Chem. Enviro.*, 6 (2024) 100104.

[3] R.F. Abbas, M.J.M. Hassan and A.M. Rheima, "Magnetic solid-phase extraction of Fast Green dye based on magnetic nanoparticles (GO/Co_3O_4/Fe_3O_4) prepared by photo-irradiation method", *Green Anal. Chem.*, 7 (2023) 100086.

[4] F. Haq et al., "Doped Magnetic Nanoparticles: From Synthesis to Applied Technological Frontiers", *Colloids Surf. B: Biointerfaces*, 247 (2024) 114410.

[5] C.L. Warner et al., "Manganese doping of magnetic iron oxide nanoparticles: tailoring surface reactivity for a regenerable heavy metal sorbent", *Langmuir*, 28(8) (2012) 3931-3937.

[6] N.T. Tasnim et al., "The promise of metal-doped iron oxide nanoparticles as antimicrobial agent", *ACS Omega*, 9(1) (2023) 16-32.

[7] Z.E. Gahrouei, S. Labbaf and A. Kermanpur, "Cobalt doped magnetite nanoparticles: synthesis, characterization, optimization and suitability evaluations for magnetic hyperthermia applications", *Physica E: Low-dimen. Syst. Nanostruct.*, 116 (2020) 113759.

[8] A.G. Leonel et al., "Tunable magnetothermal properties of cobalt-doped magnetite–carboxy methyl cellulose ferro fluids: smart nanoplatforms for potential magnetic hyperthermia applications in cancer therapy", *Nanoscale Adv.*, 3(4) (2021) 1029-1046.

[9] Z.L. Low et al., "Ultrasonic cavitation: An effective cleaner and greener intensification technology in the extraction and surface modification of nanocellulose", *Ultrason. Sonochem.*, 90 (2022) 106176.

[10] P. Adamou et al., "Recent progress on sonochemical production for the synthesis of efficient photocatalysts and the impact of reactor design", *Ultrason. Sonochem.*, 100 (2023) 106610.

[11] G. Matyszczak et al., "Sonochemical Synthesis of Low-Dimensional Nanostructures and Their Applications—A Review", *Materials*, 17(22) (2024) 5488.

[12] G. Yang et al., "Understanding the relationship between particle size and ultrasonic treatment during the synthesis of metal nanoparticles", *Ultrason. Sonochem.*, 73 (2021) 105497.

[13] A. Fuentes-García, A.C. Alavarse and A.C.M. Maldonado, "Simple sonochemical method to optimize the heating efficiency of magnetic nanoparticles for magnetic fluid hyperthermia", *ACS Omega,* 5 (2020) 26357–26364.

[14] M.S. Alkathy et al., "Effect of defects on the band gap and photoluminescence emission of Bi and Li co-substituted barium strontium titanate ceramics", *Mater. Chem. Phys.*, 275 (2022) 125235.

[15] M. Aghazadeh and M.R. Ganjali, "One-pot electrochemical synthesis and assessment of super-capacitive and super-paramagnetic performances of Co^{2+} doped Fe_3O_4 ultra-fine particles", *J. Mater. Sci.: Mater. in Electron.*, 29 (2018) 2291-2300.

[16] R.M. Cornell and U. Schwertmann, **"The iron oxides: structure, properties, reactions, occurrences, and uses"**, Vol. 664, Wiley-VCH (Weinheim, 2003), p. 536.

[17] K.S. Krane, **"Modern Physics"**, John Wiley & Sons (2019), p. 82.

[18] W.D. Shafer and G. Jacobs, **"Iron and Cobalt Catalysts"**, MDPI (2020), p. 63.

[19] V.D. Hodoroaba, "Energy-dispersive X-ray spectroscopy (EDS)", in **"Characterization of Nanoparticles"**, Elsevier (2020), pp. 397-417.

[20] A. Bengtson, D. Morgan and and U. Becker, "Spin state of iron in Fe_3O_4 magnetite and h-Fe_3O_4", *Phys. Rev. B: Cond. Matter Mater. Phys.*, 87(15) (2013) 155141.

[21] T. Muller-Reichert and G. Pigino, **"Three-Dimensional Electron Microscopy",** Academic Press (2019).

[22] R. Nandee et al., "Surface topography and surface morphology of graphene nanocomposite by FESEM, EDX and AFM analysis", *Nano-Struct. Nano-Objects*, 38 (2024) 101170.

[23] K.N. Shinde et al., "Basic mechanisms of photoluminescence", Ch.2, in **"Phosphate Phosphors for Solid-State Lighting"**, Springer (2012) 41-59.

[24] J. Liqiang et al., "Review of photoluminescence performance of nano-sized semiconductor materials and its relationships with photocatalytic activity", *Sol. Ener. Mater. Solar Cells*, 90(12) (2006) 1773-1787.

[25] P.M. Cardoso, G.J. de Moreno and S.G. Pachuca, "Effect of Cobalt Dopants on Magneto-Optic Conversion of Magnetite Nanostructures", *Iraqi J. Appl. Phys. Lett.*, 8(1) (2025) 27-30

[26] B. Bonelli et al., **"Photocatalysts for Organics Degradation"**, MDPI (2020), p. 53.

